

Spatial Structure of Au₈: Importance of Basis Set Completeness and Geometry Relaxation

Martin Diefenbach and Kwang S. Kim*

Center for Superfunctional Materials, Department of Chemistry, Pohang University of Science and Technology, San 31, Hyojadong, Namgu, Pohang 790-784, Korea

Received: August 3, 2006; In Final Form: August 24, 2006

The relative stabilities of the lowest energy structures are calculated for the gold octamer, Au₈, employing highly correlated ab initio methods. The question of dimensionality of these clusters is addressed, and a guideline for future structural studies of such systems is provided. In particular, the importance of geometry relaxation beyond the MP2 level of theory as well as the need for basis sets toward the complete limit (CBS) are discussed. The planar *D*_{4h} symmetric structure of Au₈ is the lowest energy structure. At the CCSD(T)/CBS limit, it is separated by 16 kJ mol⁻¹ from the next higher *T*_d symmetric isomer.

1. Introduction

Gold has been a fascinating material in human history due to its luster, malleability, nonreactivity, and noncorrosive durability. Nowadays, gold chemistry plays a very important role in nanoelectronics and bionanoscience.^{1–14} In particular, the structural change of gold such as clusters, nanowires, nanotubes, and nanofilms has been an intriguing subject to understand the malleability.^{15–20} Thus, one of the most fundamental issues in gold chemistry is the structural change as the gold cluster size increases. Since the 5d and 6s orbital overlap in gold^{21–23} enhances the ductility, Au₃⁻ favors a linear structure, and small anionic gold clusters (up to the 13-mer or so) show planar structures.²⁴ In the neutral state, the linearity and planarity of gold clusters are slightly reduced than those in the anionic state, but such trends are still very strong.

The structural changes from the planar or 2-dimensional (2D) to the 3-dimensional (3D) geometry would affect the gold chemistry with respect to the chemical reactivity such as oxidation/corrosion. Although small and medium size gold clusters are at the forefront of surface chemistry and catalysis^{25–32} as well as on nanoelectronics,^{33–36} the spatial structure—one of the most fundamental properties of such species—is still not unequivocally solved. It has recently been reported that the octamer Au₈ plays an outstanding role as the smallest gold cluster being an active oxidation mediator.³² In this case, Au₈ is supported on an oxide substrate and interacting with CO, distorting the spatial as well as the electronic structure³⁰ of the isolated cluster. However, it is controversial whether the structure of the pure cluster Au₈ is 2D or 3D. Until now, there have been many reports to predict and identify the turnover point from planarity to 3-dimensional frameworks for increasing cluster size (see, e.g., refs 24 and 37–40), where computational methods employed range from first-principle plane-wave density functional theory (DFT) to correlated ab initio theory at the coupled cluster level. The debate about this property has thus been narrowed down to a few particular cluster sizes, and according to ab initio calculations at the Møller–Plesset and coupled cluster levels of theory,^{24,37,41} the octamer Au₈ marks a pivotal point. Here, predictions for 2D and 3D ground-state isomers diverge depending on the level of theory applied.

Au clusters being highly correlated species involving dispersive d-shell interactions are computationally demanding to describe. While DFT provides an implicit treatment of electron correlation at low computational cost, quantitative prediction of properties for such systems is often limited due to the inherent lack of dispersion interaction. Another problem is posed by the lack of systematic improvement of quality due to the unknown exchange–correlation functional. Therefore, though there are numerous discussions on gold clusters based on DFT, our focus of attention lies upon accurate ab initio theory, which can clarify the dimensional issue of the gold cluster.

Au₈ has been predicted to be planar at most DFT levels, while the second-order Møller–Plesset (MP2) level predicts that it is 3D. However, coupled cluster expansions with singles, doubles (CCSD),²⁴ and perturbative triples excitations (CCSD(T))⁴¹ in conjunction with small basis sets yields that the 2D and 3D structures are nearly isoenergetic (slightly in favor of 2D). According to the recent efforts of Olson et al.,³⁷ their most reliable predictions yield four Au₈ isomers within 20 kJ mol⁻¹ (though slightly in favor of 3D) at the CCSD(T) level of theory. They, however, consider these results are not fully conclusive due to the basis set incompleteness and the lack of (systematic) improvement.

Since the DFT, MP2, CCSD, and CCSD(T) levels of theory give different results, a clear definitive answer is required to give a guideline for future structural studies. Owing to the recent vigorous development in nanotechnology, numerous studies on the structures of various metal clusters have been carried out based on DFT and MP2 calculations without considering the validity of the results. In this regard, it would be useful to compare the complete basis set (CBS) limit of CCSD(T) calculations on the optimized geometries with any experimental values available. Thus, in this contribution, we aim at resolving the ground-state structure of Au₈ by considering the four isomers which were previously identified as candidates for the lowest energy structure, i.e., the planar *D*_{4h} structure and the 3-dimensional *T*_d, *D*_{2d}, and *C*_s isomers (Figure 1).

2. Computational Details

Au was described by using different relativistic pseudopotentials (PP), all of which replace the [Kr]4d¹⁰4f¹⁴ 60 e⁻ core, such that the 19 e⁻ 5s²5p⁶5d¹⁰6s¹ valence space is treated

* Address correspondence to this author. E-mail: kim@postech.ac.kr.
Fax: +82-54-279-8137.

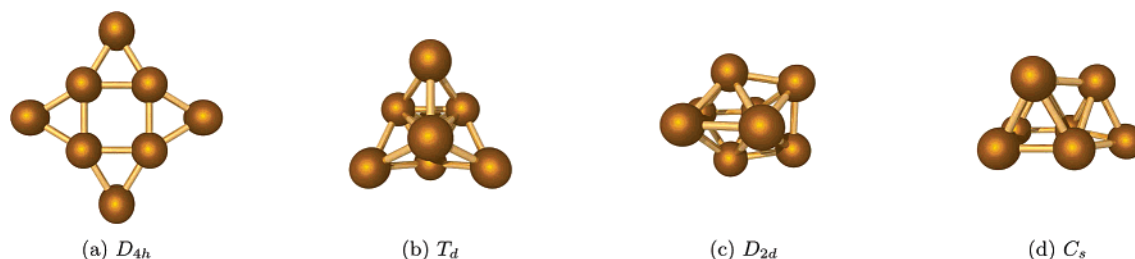


Figure 1. Planar (a) and 3-dimensional (b–d) lowest energy isomers of Au_8 .

explicitly. The various PP/basis set combinations employed correspond to the following abbreviations. SBKJC: PP of ref 42 in conjunction with the corresponding (7s7p5d)/[4s4p3d] basis set; addition of one f polarization function yields SBKJC+f,³⁷ the uncontracted set together with three f and two g functions results in SBKJC+3f2g.³⁷ MDF: PP of ref 43 with the corresponding (8s6p5d)/[7s3d4d] valence basis set; addition of two f and one g functions according to ref 44 is labeled MDF+2fg. MCDHF: PP of ref 45 in combination with the corresponding (12s12p9d3f2g)/[6s6p4d3f2g] basis set; addition of one h function (exponent = 1.380) gives MCDHF+h; the correlation consistent sets cc-pVDZ-PP to cc-pV5Z-PP⁴⁶ are also used in conjunction with the MCDHF PP.

DFT and MP2 geometry optimizations were carried out with use of the Gaussian03 package.⁴⁷ For higher correlated methods, i.e., coupled cluster theory including single and double excitations (CCSD) and perturbative triple excitation contributions (CCSD(T)), multireference perturbation theory (CASPT2), and multireference averaged quadratic coupled cluster theory (MR-AQCC), we employed the Molpro package.⁴⁸ In all calculations, the 5s5p semicore was included in the correlation treatment.

Clusters larger than Au_2 were optimized at the MP2/MDF+2fg level as well as at the CCSD(T)/MCDHF level. For the latter, we used a scaling approach, in which the coordinates of the optimized MP2/MDF+2fg structures were scaled at factors of 1.000, 1.025, and 1.050. A polynomial fit through these three points yields a minimum for the relaxed scaled structure, at which the final CCSD(T)/MCDHF energy is calculated. Although the reliability of this approach decreases with increasing degrees of freedom, the geometries obtained as such are expected to be quite accurate. For example, the difference in energy for Au_4 between a fully optimized and a relaxed structure from this scaled relaxation approach amounts to a mere 7.6 $\mu\text{hartree}$ (0.02 kJ mol^{-1}).

CBS limits were extrapolated utilizing the formula⁴⁶ $E_n = E_{\text{CBS}} + Ae^{-(n-1)} + Be^{-(n-1)^2}$, where n is the cardinal number of the basis set, i.e., $n = 2$ for double- ζ , up to $n = 5$ for quintuple- ζ . While spin–orbit effects are small for closed shell systems such as the ones considered in this study, they cancel out in relative energies for different isomers.

Calculations at the coupled cluster level of theory are computationally extensive, which involve up to ≈ 800 basis contractions (Au_8 at the cc-pVQZ-PP level) and up to half a billion configuration state functions (Au_8 (C_s) at the MCDHF level).

3. Results and Discussion

First, the geometries of the planar D_{4h} and the nonplanar T_d isomers of Au_8 are compared, as these are the lowest energy structures at the coupled cluster level predicted by Lee et al.²⁴ and Han⁴¹ (D_{4h}) and Olson et al.³⁷ (T_d). These studies used MP2 geometries to calculate coupled cluster single points with moderate basis sets. A point that deserves further attention is

TABLE 1: Single Point Calculations for Planar (D_{4h}) and Nonplanar (T_d) Structures of Au_8 at MP2/MDF+2fg Geometries^a

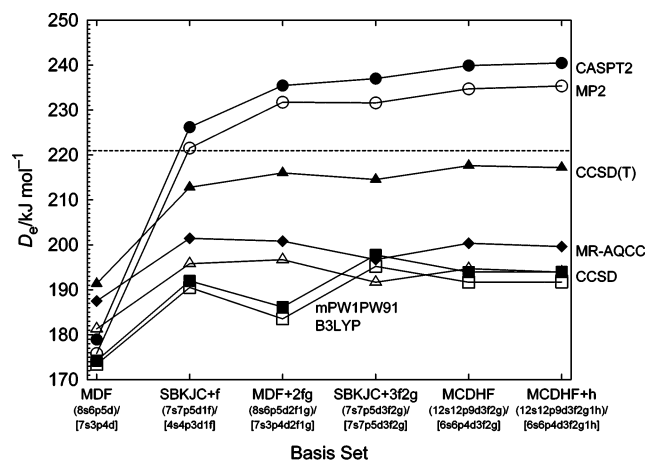
	ΔE (kJ mol^{-1})	
	MDF+2fg	MCDHF
HF	160.2	152.7
MP2	−153.3	−70.2
CCSD	−6.5	67.7
CCSD(T)	−44.9	30.7
B3LYP	82.3	86.1

^a ΔE is defined as the relative energy with respect to the D_{4h} structure, i.e., $E_{\text{rel}}(D_{4h}) = 0.0 \text{ kJ mol}^{-1}$. DFT values optimized at the B3LYP/MDF+2fg level are given for comparison.

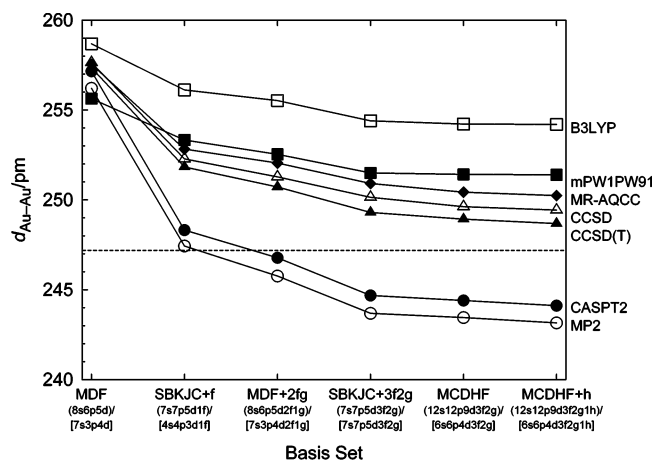
the inclusion of core–valence correlation effects—a nonnegligible factor for the description of the dispersion interaction between the gold d shells.⁴⁹

Table 1 thus displays relative energies *including* correlation of the 5s5p semicore electrons for the two species, optimized at the MP2 level by using a medium sized basis set (MDF+2fg). In addition, single points employing a more flexible expansion (MCDHF) are shown. Solely for comparison, DFT values optimized at the B3LYP/MDF+2fg level are also included. According to these data, the results are not quite converged with respect to the relative stabilities of the two isomers. While, for example, at the CCSD(T)/MDF+2fg level of theory the three-dimensional T_d structure is favored by 45 kJ mol^{-1} , at the CCSD(T)/MCDHF level of theory it is the planar D_{4h} structure that is favored by 31 kJ mol^{-1} . Apparently, with the larger basis set, each correlated method recovers 70–80 kJ mol^{-1} of correlation energy in favor of the planar structure—also note that there is no smooth convergence among the methods, but there is fluctuation, i.e., ΔE rises from MP2 to CCSD but drops again from CCSD to CCSD(T), and that DFT generally favors the 2D isomer.

To check the general convergence behavior, we calculated the gold dimer at various levels of theory employing popular PP/basis set combinations, see Figure 2. Here, however, at least at the CCSD(T) level, already basis sets including just a single f polarization function are more or less near a convergence limit for thermochemical data (Figure 2a), and larger basis sets do not change the overall picture. For the geometries, on the other hand, saturation occurs much later (Figure 2b). Remarkably, the MP2 data from the SBKJC+f PP/basis set combination, which Olson et al. also have used in their recent efforts to calculate Au_8 ,³⁷ are right on the spot for the dimer—if the dimer case were directly transferable to the higher homologues, then the MP2/SBKJC+f level of theory would be the ultimate choice. This is, however, unlikely to be the case. Rather, higher clusters are quite different from Au_2 with respect to electron correlation. Furthermore, the MP2 geometries are very different from the CCSD(T) ones. Therefore, both the relative energy and the shape of an MP2 potential energy surface are not appropriate for Au cluster energetics: For an accurate description of Au clusters,



(a) Binding energy.



(b) Equilibrium bond distance.

Figure 2. Basis set effect on binding energies and geometries of Au₂, calculated at hybrid density functional (B3LYP, mPW1PW91), correlated single reference (MP2, CCSD, CCSD(T)), multireference perturbation (CASPT2), and size-consistent multireference configuration interaction (MR-AQCC) levels. Dashed lines indicate experimental values.

TABLE 2: Calculated CCSD(T) Properties (equilibrium bond distance $d_{\text{Au-Au}}$, dissociation energy D_e , vertical ionization energy IE) of Au₂, Au₄, and Au₆ as a Function of Basis Set^a

	Au ₂ (D_{expt})			Au ₄ (D_{2h})	Au ₆ (D_{3h})
	$d_{\text{Au-Au}}$ (pm)	D_e (kJ mol ⁻¹)	IE (eV)	IE (eV)	IE (eV)
cc-pVDZ-PP	250.8	208.0	9.051	7.696	8.365
cc-pVTZ-PP	249.7	209.5	9.272	7.839	8.532
cc-pVQZ-PP	248.6	214.4	9.382	7.951	8.613
cc-pV5Z-PP	248.2	217.4	9.434		
MCDHF	248.8	217.6	9.421	7.964	8.638
CBS	247.9	218.4	9.457	7.961	8.662
exptl	247.2 ^b	222.5 ± 0.5 ^c	9.5 ± 0.3 ^d		

^a CBS extrapolation was done with the correlation consistent sets (up to cc-pV5Z-PP), for Au₄ and Au₆ (up to cc-pVQZ-PP) at scaled CCSD(T)/MCDHF geometries (see text); scale factors are 1.0203 for Au₄ and 1.0218 for Au₆. ^b Reference 50. ^c Reference 51 (D_0). ^d Reference 52.

the CCSD(T)/MP2 approach does not seem justified. Also note that multireference variants of MP2 (CASPT2) or CCSD (MR-AQCC) do not provide significant further benefit.

Evidently, geometrical and electron correlation effects play a crucial role, even more so as the size of the system increases. As to the different results for Au₈ from different calculations, the fluctuations and uncertainties in the available published data, which depend on the method and basis set used, remain so far. Since, according to Olson et al.,³⁷ Au₈ may be described by a single configuration wave function, multireference treatments will most likely also not improve the picture. Further improvement of the correlation treatment must therefore involve examination of basis set convergence as well as of geometry relaxation at the CCSD(T) level.

To this end, we estimate the quality of the MCDHF basis set by evaluating the CBS limit values for properties of smaller gold clusters. The data in Table 2 are compiled by using the very recently developed correlation consistent sets of Peterson and Puzarini.⁴⁶ The geometries of the gold dimer were fully optimized, and those of the higher homologues have been obtained from a polynomial fit to CCSD(T)/MCDHF points via scaling the coordinates of the MP2/MDF+2fg structures (see the Computational Details section), and are thus “relaxed” at the CCSD(T)/MCDHF level. In general, the MCDHF values are approximately of cc-pVQZ quality (Au–Au distance) or

TABLE 3: Relative Energies (kJ mol⁻¹) of the Four Au₈ Isomers, Calculated at the CCSD(T) Level of Theory at Relaxed MCDHF Geometries (see text)^a

basis	D_{4h}	T_d	D_{2d}	C_s
MCDHF-sp ^b	0.0	30.7	39.6	47.1
MCDHF ^c	0.0	12.6	21.5	32.2
cc-pVTZ-PP ^c	0.0	19.2	24.1	
cc-pVQZ-PP ^c	0.0	17.8	26.2	
CBS ^c	0.0	15.7	26.5	

^a CBS limits are obtained from cc-pVDZ-PP up to cc-pVQZ-PP calculations. ^b Single points calculated at unscaled MP2/MDF+2fg geometries. ^c Scale factors are 1.0213, 1.0311, 1.0313, and 1.0301, for D_{4h} , T_d , D_{2d} , and C_s , respectively.

even better, and they are thus close to the CBS limit. Therefore, the CCSD(T)/MCDHF level of theory is a very well-balanced choice.

Table 3 shows relative energies of the four Au₈ isomers with the relaxed geometries at the scaled CCSD(T)/MCDHF level. CCSD(T) single points at MP2/MDF+2fg geometries are also given for comparison. First of all, geometry relaxation lowers the relative energies of the 3D structures by about 18 kJ mol⁻¹ with respect to the planar isomer. Nevertheless, the planar D_{4h} structure is consistently the lowest energy isomer at all levels of theory. Furthermore, the T_d structure is consistently about 9 kJ mol⁻¹ lower in energy than the D_{2d} one. According to these data, a planar Au₈ structure is separated from 3D congeners by about 16 kJ mol⁻¹. Further optimization to fully relaxed geometries at the CCSD(T)/MCDHF level is not expected to change this energetic ordering of 2D vs 3D isomers, since the difference is expected to be several orders of magnitude smaller, e.g., $\Delta E_{\text{Au}_8}^{\text{MCDHF}}(\text{opt-scaled}) = 7.6 \mu\text{hartree} = 0.02 \text{ kJ mol}^{-1}$. Also, zero-point vibrational energy (ZPE) corrections are not expected to affect this general picture. At the DFT level of theory, for example, the largest difference in ZPE for the relaxed CCSD(T)/MCDHF geometries amounts to 0.6 kJ mol⁻¹ (D_{2d} (9.4 kJ mol⁻¹) vs D_{4h} (10.0 kJ mol⁻¹)).

We note that the estimated CCSD(T) results of Han⁴¹ approach this picture surprisingly well: a T_d structure is separated by $\approx 19 \text{ kJ mol}^{-1}$ from the planar D_{4h} ground-state structure. However, the energetic ordering is different, such that the T_d structure is not the first higher isomer. We also note that the planar ground state structure is in basic agreement with experimentally observed ionization energies (IEs). In their experimental study,⁵³ Jackschath et al. provide rough upper

limits of vertical ionization energies (error bars are not given), which are determined from appearance energy (AE) estimates. Thus, at the CCSD(T)/MCDHF level, the calculated IE for the planar D_{4h} isomer (8.344 eV) is closer to the rough experimental estimate (8.65 eV) than is the prediction for the T_d isomer (8.097 eV).

4. Concluding Remarks

In this contribution we have provided a systematic route to predict Au cluster energetics reliably. Au_8 is a planar, D_{4h} symmetric species. A 3-dimensional T_d structure is in close energetic vicinity. We note that this is yet another example for the diverging trends in DFT and MP2 calculations (see, e.g., refs 54 and 55); in general, DFT tends to be slightly biased in favor of 2D over 3D structures, whereas MP2 tends to be slightly biased in favor of 3D over 2D structures, while CCSD(T) tends to lie between the two cases. The present work would serve as a guideline for future structural studies on numerous metal clusters as well as for the interpretation of the presently reported results.

Acknowledgment. This work was supported by the Global Research Laboratory (GRL) project of KOSEF, by BK21, and by the Postech research project. All calculations were performed on the IBM p690 series Regatta nodes of the KISTI Supercomputing Center, Daejeon.

References and Notes

- (1) Schmidbaur, H., Ed. *Gold—Progress in Chemistry, Biochemistry and Technology*; John Wiley & Sons: Chichester, U.K., 1999.
- (2) Pyykkö, P. *Chem. Rev.* **1997**, *97* (3), 597–636.
- (3) Fernández, E. J.; Gimeno, M. C.; Laguna, A.; de Luzuriaga, J. M. L.; Monge, M.; Pyykkö, P.; Sundholm, D. *J. Am. Chem. Soc.* **2000**, *122* (30), 7287–7293.
- (4) Pyykkö, P.; Runeberg, N. *Angew. Chem., Int. Ed.* **2002**, *41* (12), 2174–2176.
- (5) Pyykkö, P.; Zhao, Y. *Angew. Chem., Int. Ed. Engl.* **1991**, *30* (5), 604–605.
- (6) Legoas, S. B.; Galvão, D. S.; Rodrigues, V.; Ugarte, D. *Phys. Rev. Lett.* **2002**, *88* (7), 76105/1–4.
- (7) Rubio-Bollinger, G.; Bahn, S. R.; Agraït, N.; Jacobsen, K. W.; Vieira, S. *Phys. Rev. Lett.* **2001**, *87* (2), 26101/1–4.
- (8) Rodrigues, V.; Ugarte, D. *Nanotechnology* **2002**, *13* (3), 404–408.
- (9) Mozos, J. L.; Ordejón, P.; Brandbyge, M.; Taylor, J.; Stokbro, K. *Nanotechnology* **2002**, *13* (3), 346–351.
- (10) Todorov, T. N.; Hoekstra, J.; Sutton, A. P. *Phys. Rev. Lett.* **2001**, *86* (16), 3606–3609.
- (11) Rodrigues, V.; Ugarte, D. *Phys. Rev. B* **2001**, *63* (7), 73405/1–4.
- (12) Sánchez-Portal, D.; Artacho, E.; Junquera, J.; Ordejón, P.; García-Li, A.; Soler, J. M. *Phys. Rev. Lett.* **1999**, *83* (19), 3884–3887.
- (13) Landman, U.; Luedtke, W. D.; Salisbury, B. E.; Whetten, R. L. *Phys. Rev. Lett.* **1996**, *77* (7), 1362–1365.
- (14) Yanson, A. I.; Bollinger, G. R.; van den Brom, H. E.; Agraït, N.; van Ruitenbeek, J. M. *Nature* **1998**, *395* (6704), 783–785.
- (15) Bauschlicher, C. W., Jr.; Langhoff, S. R.; Partridge, H. *J. Chem. Phys.* **1989**, *91* (4), 2412–2419.
- (16) Partridge, H.; Bauschlicher, C. W., Jr.; Langhoff, S. R. *Chem. Phys. Lett.* **1990**, *175* (5), 531–535.
- (17) Schmidt, M.; Kusche, R.; von Issendorff, B.; Haberland, H. *Nature* **1998**, *393* (6682), 238–240.
- (18) Häkkinen, H.; Moseler, M.; Landman, U. *Phys. Rev. Lett.* **2002**, *89* (3), 33401/1–4.
- (19) Gilb, S.; Weis, P.; Furche, F.; Ahlrichs, R.; Kappes, M. M. *J. Chem. Phys.* **2002**, *116* (10), 4094–4101.
- (20) Bonaëia-Koutecký, V.; Burda, J.; Mitrić, R.; Ge, M.; Zampella, G.; Fantucci, P. *J. Chem. Phys.* **2002**, *117* (7), 3120–3131.
- (21) Geng, W. T.; Kim, K. S. *Phys. Rev. B* **2003**, *67* (23), 233403/1–4.
- (22) Nautiyal, T.; Youn, S. J.; Kim, K. S. *Phys. Rev. B* **2003**, *68* (3), 33407/1–4.
- (23) Lee, H. M.; Diefenbach, M.; Suh, S. B.; Tarakeshwar, P.; Kim, K. S. *J. Chem. Phys.* **2005**, *123* (7), 74328/1–5.
- (24) Lee, H. M.; Ge, M.; Sahu, B. R.; Tarakeshwar, P.; Kim, K. S. *J. Phys. Chem. B* **2003**, *107* (37), 9994–10005.
- (25) Pyykkö, P. *Angew. Chem., Int. Ed.* **2004**, *43* (34), 4412–4456.
- (26) Schwerdtfeger, P. *Angew. Chem., Int. Ed.* **2003**, *42* (17), 1892–1895.
- (27) Bulusu, S.; Li, X.; Wang, L.-S.; Zeng, X. C. *Proc. Natl. Acad. Sci. U.S.A.* **2006**, *103* (22), 8326–8330.
- (28) Ji, M.; Gu, X.; Li, X.; Gong, X.; Li, J.; Wang, L.-S. *Angew. Chem., Int. Ed.* **2005**, *44* (43), 7119–7123.
- (29) Li, J.; Li, X.; Zhai, H.-J.; Wang, L.-S. *Science* **2003**, *299* (5608), 864–867.
- (30) Häkkinen, H.; Abbet, S.; Sanchez, A.; Heiz, U.; Landman, U. *Angew. Chem., Int. Ed.* **2003**, *42* (11), 1297–1300.
- (31) Fielicke, A.; von Helden, G.; Meijer, G.; Pedersen, D. B.; Simard, B.; Rayne, D. M. *J. Am. Chem. Soc.* **2005**, *127* (23), 8416–8423.
- (32) Yoon, B.; Häkkinen, H.; Landman, U.; Wörz, A. S.; Antonietti, J.-M.; Abbet, S.; Judai, K.; Heiz, U. *Science* **2005**, *307* (5708), 403–407.
- (33) Zheng, J.; Petty, J. T.; Dickson, R. M. *J. Am. Chem. Soc.* **2003**, *125* (26), 7780–7781.
- (34) Basch, H.; Ratner, M. A. *J. Chem. Phys.* **2005**, *123* (23), 234704/1–19.
- (35) Dadosh, T.; Gordin, Y.; Krahne, R.; Khivrich, I.; Mahalu, D.; Frydman, V.; Sperling, J.; Yacoby, A.; Bar-Joseph, I. *Nature* **2005**, *436* (4), 677–680.
- (36) Cui, X. D.; Primak, A.; Zarate, X.; Tomfohr, J.; Sankey, O. F.; Moore, A. L.; Moore, T. A.; Gust, D.; Harris, G.; Lindsay, S. M. *Science* **2001**, *294* (5542), 571–574.
- (37) Olson, R. M.; Varganov, S.; Gordon, M. S.; Metiu, H.; Chretien, S.; Piecuch, P.; Kowalski, K.; Kucharski, S. A.; Musial, M. *J. Am. Chem. Soc.* **2005**, *127* (3), 1049–1052.
- (38) Walker, A. V. *J. Chem. Phys.* **2005**, *122* (9), 94310/1–12.
- (39) Remacle, F.; Kryachko, E. S. *J. Chem. Phys.* **2005**, *122* (4), 44304/1–14.
- (40) Grönbeck, H.; Broqvist, P. *Phys. Rev. B* **2005**, *71* (7), 73408/1–4.
- (41) Han, Y.-K. *J. Chem. Phys.* **2006**, *124* (2), 24316/1–3.
- (42) Stevens, W. J.; Krauss, M.; Basch, H.; Jasien, P. G. *Can. J. Chem.* **1992**, *70* (2), 612–630.
- (43) Schwerdtfeger, P.; Dolg, M.; Schwarz, W. H. E.; Bowmaker, G. A.; Boyd, P. D. W. *J. Chem. Phys.* **1989**, *91* (3), 1762–1774.
- (44) Martin, J. M. L.; Sundermann, A. *J. Chem. Phys.* **2001**, *114* (8), 3408–3420.
- (45) Figgen, D.; Rauhut, G.; Dolg, M.; Stoll, H. *Chem. Phys.* **2005**, *311* (1–2), 227–244.
- (46) Peterson, K. A.; Puzzarini, C. *Theor. Chem. Acc.* **2005**, *114* (4–5), 283–296.
- (47) Frisch, M. J.; Trucks, G. W.; Schlegel, H. B.; Scuseria, G. E.; Robb, M. A.; Cheeseman, J. R.; Montgomery, J. A., Jr.; Vreven, T.; Kudin, K. N.; Burant, J. C.; Millam, J. M.; Iyengar, S. S.; Tomasi, J.; Barone, V.; Mennucci, B.; Cossi, M.; Scalmani, G.; Rega, N.; Petersson, G. A.; Nakatsuji, H.; Hada, M.; Ehara, M.; Toyota, K.; Fukuda, R.; Hasegawa, J.; Ishida, M.; Nakajima, T.; Honda, Y.; Kitao, O.; Nakai, H.; Klene, M.; Li, X.; Knox, J. E.; Hratchian, H. P.; Cross, J. B.; Adamo, C.; Jaramillo, J.; Gomperts, R.; Stratmann, R. E.; Yazyev, O.; Austin, A. J.; Cammi, R.; Pomelli, C.; Ochterski, J. W.; Ayala, P. Y.; Morokuma, K.; Voth, G. A.; Salvador, P.; Dannenberg, J. J.; Zakrzewski, V. G.; Dapprich, S.; Daniels, A. D.; Strain, M. C.; Farkas, O.; Malick, D. K.; Rabuck, A. D.; Raghavachari, K.; Foresman, J. B.; Ortiz, J. V.; Cui, Q.; Baboul, A. G.; Clifford, S.; Cioslowski, J.; Stefanov, B. B.; Liu, G.; Liashenko, A.; Piskorz, P.; Komaromi, I.; Martin, R. L.; Fox, D. J.; Keith, T.; Al-Laham, M. A.; Peng, C. Y.; Nanayakkara, A.; Challacombe, M.; Gill, P. M. W.; Johnson, B.; Chen, W.; Wong, M. W.; Gonzalez, C.; Pople, J. A. *Gaussian 03*, rev. C.02; Gaussian Inc., Wallingford, CT, 2004.
- (48) Werner, H.-J.; Knowles, P. J.; Lindh, R.; Schütz, M.; Celani, P.; Korona, T.; Manby, F. R.; Rauhut, G.; Amos, R. D.; Bernhardsson, A.; Berning, A.; Cooper, D. L.; Deegan, M. J. O.; Dobbyn, A. J.; Eckert, F.; Hampel, C.; Hetzer, G.; Lloyd, A. W.; McNicholas, S. J.; Meyer, W.; Mura, M. E.; Nicklass, A.; Palmieri, P.; Pitzer, R.; Schumann, U.; Stoll, H.; Stone, A. J.; Tarroni, R.; Thorsteinsson, T. *Molpro* Version 2002.6, 2002.
- (49) Hess, B. A.; Kaldor, U. *J. Chem. Phys.* **2000**, *112* (4), 1809–1813.
- (50) Huber, K. P.; Herzberg, G. In *NIST Chemistry WebBook, NIST Standard Reference Database*; Linstrom, P. J., Mallard, W. G., Eds.; National Institute of Standards and Technology: Gaithersburg, MD, 2001; Vol. 69.
- (51) James, A. M.; Kowalczyk, P.; Simard, B.; Pinegar, J. C.; Morse, M. D. *J. Mol. Spectrosc.* **1994**, *168* (2), 248–257.
- (52) Lias, S. G.; Bartmess, J. E.; Liebman, J. F.; Holmes, J. L.; Levin, R. D.; Mallard, W. G. In *NIST Chemistry WebBook, NIST Standard Reference Database*; Linstrom, P. J., Mallard, W. G., Eds.; National Institute of Standards and Technology: Gaithersburg, MD, 2001; Vol. 69.
- (53) Jackschath, C.; Rabin, I.; Schulze, W. *Ber. Bunsen-Ges.* **1992**, *96* (9), 1200–1204.
- (54) Singh, N. J.; Olleta, A. C.; Kumar, A.; Park, M.; Yi, H.-B.; Bandyopadhyay, I.; Lee, H. M.; Tarakeshwar, P.; Kim, K. S. *Theor. Chem. Acc.* **2006**, *115* (2–3), 127–135.
- (55) Lee, H. M.; Suh, S. B.; Lee, J. Y.; Tarakeshwar, P.; Kim, K. S. *J. Chem. Phys.* **2000**, *112* (22), 9759–9772.